

**BUREAU INTERNATIONAL
DES POIDS ET MESURES**

**Comparison of Quantum Hall Effect resistance standards
of the PTB and the BIPM**

**on-going comparison
BIPM.EM-K12**

**Report on the 2013 on-site comparison
Final Report
July 2014**

R.Goebel⁽¹⁾, N.Fletcher⁽¹⁾, B.Rolland⁽¹⁾

M.Götz⁽²⁾ and E.Pesel⁽²⁾

⁽¹⁾ Bureau International des Poids et Mesures,
Pavillon de Breteuil, Sèvres, France.

⁽²⁾ Physikalisch-Technische Bundesanstalt,
Bundesallee 100, Braunschweig, Germany.



Comparison of Quantum Hall Effect resistance standards of the PTB and the BIPM

On-going comparison BIPM.EM-K12

1 Introduction

The comparison reported here is part of a BIPM programme to verify the international coherence of primary resistance standards by comparing Quantum Hall Effect (QHE) based standards of the national laboratories with that of the BIPM. Five such comparisons have already been carried out in the period 1993 to 1999 with the BNM/LCIE (France) [1], the METAS (Switzerland) [2], the PTB (Germany) [3], the NPL (United Kingdom) [4] and the NIST (USA) [5].

A survey conducted by the BIPM in 2009 showed that a large number of NMIs are interested in participating in this programme, or in repeating the exercise. The BIPM therefore decided to start a new series of on-site comparisons, the first of them being the BIPM-PTB.

2 Principle of the comparison

The comparison includes three parts: the calibration of a 100 Ω standard resistor in terms of the Quantized Hall Resistance (QHR) standard of each laboratory, the scaling from 100 Ω to 10 k Ω and the scaling from 100 Ω to 1 Ω .

The QHR value used is the conventional value R_{K-90} .

The relative difference in the calibrations of the standard resistor of nominal value $R = 100 \Omega$ is expressed as $(R_{PTB} - R_{BIPM}) / R_{BIPM}$, where R_{BIPM} and R_{PTB} are the values attributed by the BIPM and the PTB respectively.

The ratio $K1$ is defined as the ratio $R_{10k\Omega} / R_{100\Omega}$ of the resistance of two standards of nominal values 10 k Ω and 100 Ω . The relative difference in the measurements of $K1$ is expressed as $(K1_{PTB} - K1_{BIPM}) / K1_{BIPM}$, where $K1_{PTB}$ and $K1_{BIPM}$ are the values attributed by the BIPM and the PTB respectively.

Similarly, $K2$ is defined as the ratio $R_{100\Omega} / R_{1\Omega}$ of the resistance of two standards of nominal values 100 Ω and 1 Ω . The relative difference in the measurements of $K2$ is expressed as $(K2_{PTB} - K2_{BIPM}) / K2_{BIPM}$, where $K2_{PTB}$ and $K2_{BIPM}$ are the values attributed by the BIPM and the PTB respectively.

All the results are reported with their associated standard uncertainty. The resistance value of each standard is defined as its four-terminal ‘dc-resistance’, i.e. the dc voltage to current ratio once any thermal emf across the resistor (in particular that induced by the Peltier effect [6, section 2.1.3]) has reached a stable value. Experimental results reported here show that such specification can be difficult to meet, in particular for the 1 Ω standards.

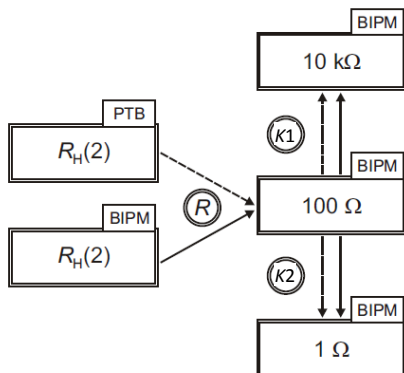


Figure 1 : Schematic of the on-site comparison performed at PTB in November 2013. The resistances to be compared are represented by rectangles, the resistance R or the ratios K to be determined by circles. Solid and dashed arrows stand for measurements with the BIPM’s 1 Hz bridge or with PTB’s CCC bridge, respectively.

3 The BIPM measurement system and the transfer standards

A complete QHE standard was taken from the BIPM to the PTB. The BIPM's transportable QHE standard includes a cryostat containing a superconducting magnet and a low-temperature insert, a set of QHE samples mounted on a cryogenic probe and a room-temperature ac resistance ratio bridge operating at 1 Hz. The bridge is equipped with two room-temperature current comparators of nominal ratios 2065/16 and 1500/15.

Three resistance standards of 1 Ω , 100 Ω and 10 k Ω were also taken from the BIPM, to be used as common standards on the BIPM and the PTB measurement facilities. They are fitted in temperature-controlled (25 $^{\circ}\text{C}$) individual enclosures.

For these conventional standards, the differences between values measured at 1 Hz and at 'dc' are small but not negligible. These differences have been determined at the BIPM prior to the comparison, using the BIPM cryogenic current comparator (CCC) operated at 'dc'. They are applied as corrections to the measurements carried out at 1 Hz, meaning that the ac bridge is used as a transfer instrument referenced to the BIPM CCC.

This method is preferable to transporting the BIPM CCC bridge itself since the ac bridge is a more rugged instrument, simple to operate, and much less sensitive to electromagnetic interference and temperature fluctuations. Furthermore, it provides resolution and reproducibility that are comparable to those of the BIPM CCC.

The main possible sources contributing to the frequency coefficients listed in Table 1 are the QHR, the 1 Hz bridge, and the conventional standards. At 1 Hz the frequency dependence of the QHR is assumed to be negligible [7] when compared with the uncertainty of the comparison, and the characterization of the bridge showed that the error at 1 Hz was smaller than 1 ppb. The frequency coefficients are therefore mainly related to the properties of the conventional standards.

Resistance ratio	Rel. corr. 1 Hz-'dc' / 10^{-6}	Standard uncertainty / 10^{-9}
$R_H(2) / 100 \Omega$	-0.0044	1.0
10 000 $\Omega / 100 \Omega$	-0.0060	1.0
100 $\Omega / 1 \Omega$	-0.0176	1.5

Table 1 : correction applied to the measurements carried out at 1 Hz (in relative terms).
These values are specific to the three standards used in this comparison.

The quantum Hall samples used by the BIPM are GaAs-based heterostructures fabricated by the Laboratoire d'Electronique Philips (LEP), of the same type as those used for previous on-site comparisons and for the comparison of quantized Hall resistance in GaAs and in graphene at NPL in 2010 [8].

A detailed description of the BIPM QHE facility and of the three conventional standards can be found in [1] [9] [10].

The BIPM uncertainty budget for the measurement of the three resistance ratios is summarized in Table 2.

Resistance ratio	$R_H(2) / 100 \Omega$	10 k Ω / 100 Ω	100 Ω / 1 Ω
Relative standard uncertainties	/ 10^{-9}	/ 10^{-9}	/ 10^{-9}
Reference CCC bridge			
Imperfect CCC winding ratio	1.0	1.0	1.0
Resistive divider calibration	0.5	0.5	0.5
Leakage resistances	0.2	0.2	-
Noise rectification in CCC	1.0	1.0	1.0
Imperfect realization of the QHR	1.0	-	-
Correction for 1 Hz-dc difference	1.0	1.0	1.5
Combined type-B std. uncertainty $u_B =$	2.1	1.8	2.1

Table 2 : BIPM uncertainty budget for the measurement of the three resistance ratios.

4 The PTB measurement system

The re-designed PTB measurement bridge (replacement of the previous version used in [3]) is based on a 12-bit CCC with 18 windings having an overall of 4647 turns [11] and a PC-controlled electronics module. The latter comprises a digital double-current source, an improved bridge-voltage detector [12] and a binary compensation unit [13].

Table 3 summarizes the main parameters chosen for the three resistance comparison settings along with the respective type-B uncertainty contributions.

Parameters	Resistance Ratio (Primary / Secondary Resistance)		
	$R_H(2) / 100 \Omega$	10 k Ω / 100 Ω	100 Ω / 1 Ω
Numbers of turns N_1 / N_2	4001 / 31	4100 / 41	200 / 2
Voltage drop $\Delta(I_2 R_2)$ in V_{pk-pk}	1.000	1.000	0.100
Compensation ratio k	-9.81×10^{-2}	-9.37×10^{-2}	6.21×10^{-3}
Relative standard uncertainty contributions	/ 10^{-9}	/ 10^{-9}	/ 10^{-9}
CCC windings ratio ^[a]	0.059	0.058	0.058
Compensation ratio k ^[b]	0.142	0.132	0.180
Bridge voltage ΔU measurement (w/o type-A)	0.200	0.152	0.619
Voltage drop $\Delta(I_2 R_2)$ measurement	0.003	< 0.001	0.008
Leakage resistances ^[c]	0.006	0.006	< 0.001
Correction of $R_H(2)$ for finite dissipation	0.018	not applied	not applied
Combined type-B std. uncertainty $u_B =$	0.25	0.21	0.65

Table 3: Parameters and type-B contributions to the uncertainty budget of the PTB measurements. The choice of a single-turn auxiliary winding included into the primary circuit is common to all three configurations.

Note that in Table 3 the type-B uncertainty of the bridge voltage includes the finite non-linearity of the voltage detector and the possible bias added to ΔU as a consequence of noise rectification in the SQUID sensor with its non-linear voltage-flux dependence.

The systematic effect of the duration of the current reversal cycle on ΔU is treated separately. This is done in terms of a low-frequency feature of the resistors to be compared, in analogy with the 1 Hz – ‘dc’ difference (see section 7).

If not stated otherwise, the measurements are performed with cycles as follows: ‘positive current plateau’, current reversal, ‘negative current plateau’, current reversal. During each plateau time (nominally 10.0 s, but effectively longer by about 15% needed for data exchange with the PC), 500 bridge voltage data points are read at a rate of 50 samples per second, but only the second half of these data enters the calculation of ΔU as described in [13]. The ramping time of the current reversals is as short as 0.2 s in all of the measurements with the PTB setup in this comparison.

For the sake of simplicity, the quantity we call cycle time T_C later in this report is just two times the nominal plateau duration, i.e., 20 s for the standard case.

Additional notes on uncertainty contributions:

- (a) The numbers given in this line of the table are based on the estimation of an upper limit for the relative winding ratio error of 1×10^{-10} ; the corresponding uncertainty is treated as one with a rectangular distribution. The purely geometry-related ratio error cannot be easily discriminated from mixing-down effects in measurements via the SQUID (the latter already enter the type-B uncertainty of ΔU as mentioned above.) A ratio error test is performed with a current I flowing through 2 CCC windings (or series combinations of several winding) with the same total numbers of turns, N , in opposition. Both effects will contribute to the measured residual signal, but the “true” geometry-related error will dominate in the limit of high NI products. As a consequence, one typically has less reliable ratio error data for windings with low numbers of turns. An earlier comprehensive set of ratio error tests revealed the following results: For 8 configurations with $N \geq 512$ and the product NI between 20 and 80 A (*peak-peak*), we found the relative ratio error to be smaller than 4×10^{-12} . For 32 configurations with N from 4 to 256 and NI between 2 to 10 A, we found a maximum relative ratio error of less than 4×10^{-11} . Finally, the corresponding value obtained for 6 configurations with $N = 1$ or 2 and NI from 0.6 to 1.2 A, was 7×10^{-11} .
- (b) The relative uncertainty of the compensation ratio is estimated to be not higher than 1×10^{-5} for any chosen k value (rectangular distribution assumed). This value holds for the chosen interval of re-calibration of the compensation unit, it also covers the influence of possible temperature changes. The uncertainties given here are calculated for the specific settings of the compensation used in these measurements.
- (c) Due to the exclusive use of PTFE as the insulating material in connectors and cables – the latter with internal screens between high- and low-potential leads [14], the isolation is very good. From experimental tests including triangular comparisons of resistors and shifting the connection to reference potential (ground) between secondary and primary circuit, we estimate a leakage resistance between high and low potential parts of the bridge of order $10^{14} \Omega$. The relative uncertainty contributions (rectangular distribution assumed) given here are calculated for the very conservative estimation of $10^{13} \Omega$ in parallel with the lower of the two resistors to be compared according to the ground connection scheme used in the measurements.

5 Measurement of the 100 Ω standard resistor in terms of $R_H(2)$

5.1 BIPM measurements

5.1.a Preliminary tests

The quantum Hall samples were operated on the $i = 2$ plateau at a temperature of 1.3 K, with a current of 40 μA rms. The magnetic flux density corresponding to the middle of the plateau was determined by recording V_{xx} as a function of magnetic flux, and was found to be 10.5 T. The two-terminal Hall resistance of the four terminal pairs of the devices was checked before and after each series of measurements, showing that the contact resistance was smaller than a few ohms (not larger than 5 Ω , measurement limited by the resolution of the DVM used).

The absence of significant longitudinal dissipation along both sides of the device was tested as described in [15] section 6.2 by combining the measurements obtained from four different

configurations of voltage contacts: two opposite pairs in the center and at the end of the sample, and two diagonal configurations. This operation takes about two hours.

The absence of longitudinal dissipation was demonstrated within 3×10^{-10} in relative terms, with a standard deviation of 5×10^{-10} . Subsequent series of measurements were taken from the central pair of contacts only.

5.1.b BIPM results

With $40 \mu\text{A}$ rms in the quantum Hall sample, the nominal current in 100Ω is 5.2 mA rms, corresponding to 2.7 mW .

In the tables below, the calibration of the resistance is expressed as the relative difference from the nominal 100Ω value: $((R_{\text{BIPM}}/100 \Omega) - 1) / 10^{-6}$

Each measurement reported in Table 4 is the mean value of five individual measurements, corresponding to a total integration time of about 26 minutes. The associated dispersion is estimated by the standard deviation of the five measurements.

On the 15 November, the 100Ω standard was connected alternately to the BIPM and to the PTB bridges, for a total of five BIPM measurements interleaved with four PTB measurements. After each change, ten minutes were allowed for thermal stabilization of the connections, with measurement current applied. Both series are shown in Figure 3.

	at 1Hz	'dc' corrected	
Time	$(R_{\text{BIPM}}/100\Omega)-1 / 10^{-6}$	$(R_{\text{BIPM}}/100\Omega)-1 / 10^{-6}$	dispersion / 10^{-9}
15:16	20.80452	20.80892	0.6
16:40	20.80326	20.80766	0.8
17:50	20.80296	20.80736	1.1
18:54	20.80306	20.80746	1.1
20:05	20.80360	20.80800	0.6
mean value =		20.8079	
Std. dev. u_A =		0.63×10^{-9}	

Table 4 : BIPM measurements of the 100Ω standard in terms of $R_H(2)$, on 15 November 2013. Results are expressed as the relative difference from the nominal 100Ω value.

BIPM result: $R_{\text{BIPM}} = 100 \times (1 + 20.8079 \times 10^{-6}) \Omega$
 Relative standard uncertainty: $u_{\text{BIPM}} = 2.2 \times 10^{-9}$
 where u_{BIPM} is calculated as the quadratic sum of $u_A = 0.63 \times 10^{-9}$ and, from Table 2, $u_B = 2.1 \times 10^{-9}$

5.2 PTB measurements

5.2.a Preliminary tests

The PTB-made GaAs-based quantum Hall sample P137-18 [16] [17] with eight Sn-ball contacts (two current and two times three voltage contacts) has been operated at a temperature of 2.2 K in a liquid helium cryostat with lambda point refrigerator. The magnetic flux density of 10.66 T corresponds to the middle of the $i = 2$ plateau as previously determined at a current level of $\pm 50 \mu\text{A}$.

To evaluate the influence of finite longitudinal dissipation, in addition to the measurement with the middle contact pair, we have performed measurements for four more configurations of voltage contacts: two opposite pairs at the ends of the sample plus two diagonal ones. Note that all these measurements are regular comparisons of the quantized Hall resistor - just with the respective pair of

voltage contacts - and a 100 Ω conventional resistor (here, the one from BIPM) at the current level $\pm 38.74 \mu\text{A}$. Together with the separately determined parameter s accounting for the ‘non-perpendicular’ Hall geometry [18], we found a ΔU -correction of $0.17 \text{ nV}_{\text{pk-pk}}$ for the given current bias level.

The total uncertainty of this correction value – resulting from the uncertainty contributions of the finite longitudinal voltage drop and of the s -parameter – is included in Table 3.

5.2.b PTB results for standard cycle duration

The results of four measurements each over 60.5 cycles of duration $T_C = 20 \text{ s}$ are presented in Table 5. The effective overall duration of the measurements of about 23 minutes is slightly shorter, but comparable to that of the BIPM measurements. The power of about 2.5 mW dissipated in the 100 Ω resistor (neglecting the reduction of power dissipation during the very short ramping time) is slightly lower, but still close to the corresponding value for the BIPM measurements.

Time	$(R_{\text{PTB}}/100\Omega) - 1$ / 10^{-6}	Dispersion / 10^{-9}
16:03	20.807 31	0.13
17:15	20.807 53	0.10
18:21	20.807 25	0.12
19:30	20.807 57	0.15
mean value =	20.807 41	
Std. dev. =	0.16×10^{-9}	

Table 5: PTB measurements of the 100 Ω standard in terms of $R_{\text{H}}(2)$, on 15 November 2013. Results are expressed as the relative difference from the nominal 100 Ω value.

PTB result: $R_{\text{PTB}} = 100 \times (1 + 20.8074 \times 10^{-6}) \Omega$
 Relative standard uncertainty: $u_{\text{PTB}} = 0.30 \times 10^{-9}$
 where u_{PTB} is calculated as the quadratic sum of
 $u_{\text{A}} = 0.16 \times 10^{-9}$ and, from Table 3, $u_{\text{B}} = 0.25 \times 10^{-9}$.

5.2.c Possible influence of the cycle duration

In a separate series of measurements performed the next day, 16 November, the cycle duration was varied in a time-symmetric manner: starting from 240.5 cycles of $T_C = 5.2$ s, followed by 120.5×10 s, 60.5×20 s, 60.5×40 s and 60.5×80 s, after that going back with reducing T_C from 60.5×40 s to 240.5×5.2 s. All these measurements were performed within about 5.5 hours; the current cycles were started about 40 minutes prior to the first measurement to allow for thermal stabilization.

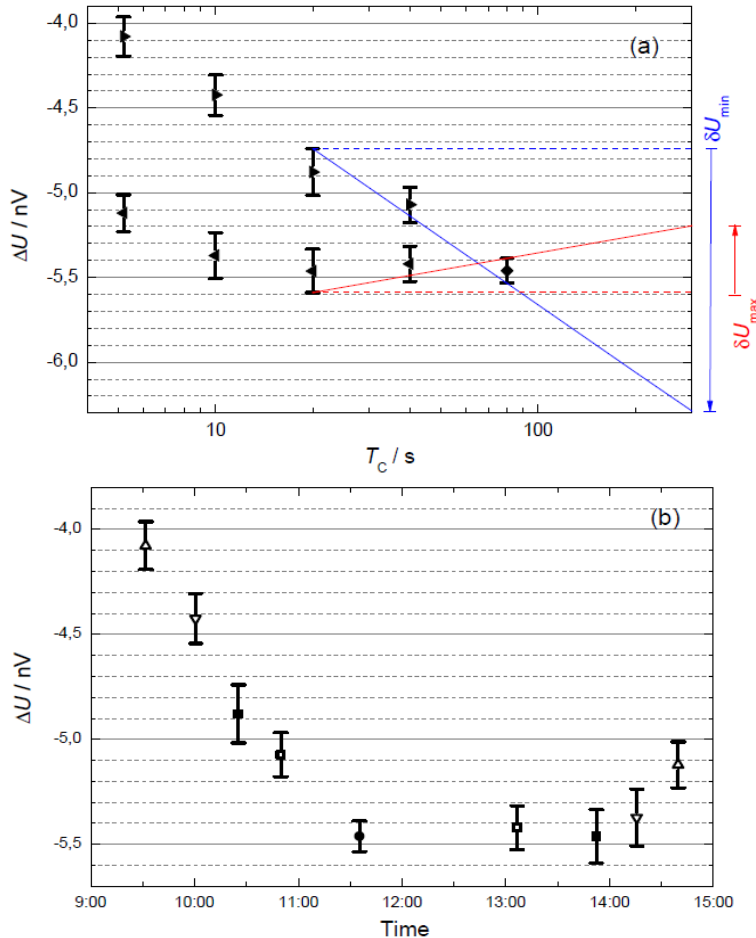


Figure 2 : Average bridge voltage difference ΔU for different cycle duration, T_C .

In panel (a), the results of the first part of the series of measurements with increasing T_C are plotted as triangles pointing to the right, the result for the maximum T_C as a diamond and finally for decreasing T_C as triangles pointing to the left.

Panel (b) shows the same results in the time order of the measurements. Same symbols stand for the same T_C . The filled symbols represent the values for $T_C = 20$ s (squares) or 80 s (circle), respectively, the data on which the extrapolations in panel (a) have been based.

The measurement results as shown in Figure 2 (a) apparently display a significant influence of T_C on ΔU for the first part of the series, but not for its second part. Starting from the pair of values obtained for the standard of 20 s or for the 80 s maximum cycle duration, respectively, linear extrapolations of ΔU in this semi-log plot provide an estimate of a correction δU potentially to be applied. For the approximately 300 s of cycle duration in case of the CCC measurements at BIPM, δU would be found in an interval from -1.55 nV to $+0.39$ nV, i.e., $\delta U = (-0.58 \pm 0.97)$ nV with a rectangular distribution. According to the negative sign of this correction, the 'dc' R_{PTB} results would be shifted towards higher values by about 0.6 parts in 10^9 .

In Figure 2 (b) the full sequence of measurement results is plotted in time order. This suggests that the variations seen in Figure 2 (b) are not in fact meaningful, but rather are the result of drifts in the resistor value during the measurement period. Variations of the order 1 or 2 parts in 10^9 over 5 hours of measurements are not surprising, and are not well rejected in this test (in contrast to the interleaved measurements main comparison result). For this reason, we decide not to apply the above result as a correction.

5.3 100 Ω measurements comparison

From Figure 3, we suggest that the stability of the resistor is such that any uncertainty contribution from possible instabilities was estimated to be negligible.

Relative difference PTB – BIPM: $(R_{\text{PTB}} - R_{\text{BIPM}}) / R_{\text{BIPM}} = -0.5 \times 10^{-9}$

Relative combined standard uncertainty: $u_{\text{comp}} = 2.2 \times 10^{-9}$

where u_{comp} is calculated as the quadratic sum of $u_{\text{BIPM}} = 2.2 \times 10^{-9}$ and $u_{\text{PTB}} = 0.30 \times 10^{-9}$

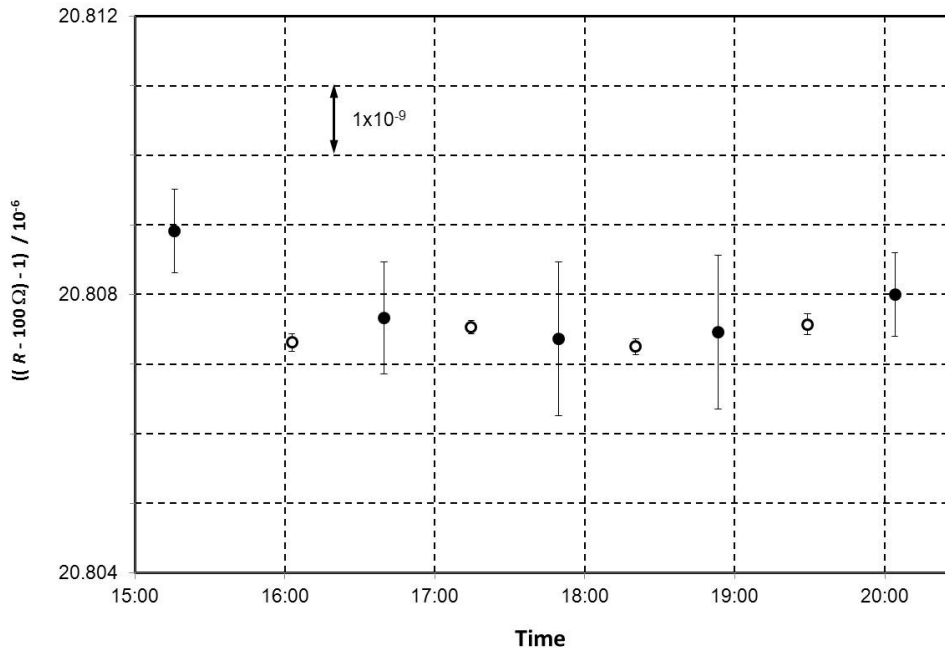


Figure 3: PTB (white circles) and BIPM (black dots) measurements of the 100 Ω resistance R in terms of $R_{\text{H}}(2)$ on 15 November 2013. The uncertainty bars correspond to the dispersion observed during each measurement.

6 Measurements of the (10 000 Ω / 100 Ω) ratio K1

6.1 BIPM measurements of K1

The measurements were carried out at 1 Hz with a 50 μA rms current in the 10 000 Ω standard. Similarly to the measurements described in section 5, each result reported in Table 6 is the mean value of 5 individual measurements, corresponding to a total integration time of about 26 minutes. The associated dispersion is estimated by the standard deviation of the mean of the five measurements. The two BIPM standards were connected alternately to the PTB and BIPM bridges: four BIPM measurements were interleaved with five PTB measurements.

	At 1Hz	'dc' corrected	
Time	$(K1_{\text{BIPM}}/100) - 1$ / 10 ⁻⁶	$(K1_{\text{BIPM}}/100) - 1$ / 10 ⁻⁶	dispersion / 10 ⁻⁹
11:34	- 22.845 80	- 22.851 80	0.5
13:03	-22.844 08	- 22.850 08	1.2
14:19	-22.845 17	- 22.851 17	0.5
15:46	-22.845 24	- 22.851 24	0.8
	mean value =	- 22.851 1	
	Std dev. of mean u_A =	0.4×10^{-9}	

Table 6 : BIPM measurements of the (10 000 Ω / 100 Ω) ratio K1 on 18 November 2013. Results are expressed as the relative difference from the nominal value 100.

BIPM result: $K1_{\text{BIPM}} = 100 \times (1 - 22.851 1 \times 10^{-6})$
 Relative standard uncertainty: $u_{\text{BIPM}} = 1.9 \times 10^{-9}$
 where u_{BIPM} is calculated as the quadratic sum of $u_A = 0.36 \times 10^{-9}$ and, from Table 2 $u_B = 1.8 \times 10^{-9}$

6.2 PTB measurements of K1

6.2.a PTB results for standard cycle duration

The PTB measurements, each 60.5 cycles of $T_C = 20$ s, with a current of ± 50 μA through the 10000 Ω standard give the five results listed in Table 7 .

Time	$(K1_{\text{PTB}}/100) - 1$ / 10 ⁻⁶	dispersion / 10 ⁻⁹
11:00	- 22.849 95	0.9
12:30	- 22.849 42	0.6
13:50	- 22.851 19	0.7
15:15	- 22.850 28	0.6
16:40	- 22.850 83	0.7
	mean value =	- 22.850 33
	Std dev.of mean u_A =	0.31×10^{-9}

Table 7 : PTB measurements of the (10 000 Ω / 100 Ω) ratio K1. Results are expressed as the relative difference from the nominal value 100.

PTB result: $K1_{\text{PTB}} = 100 \times (1 - 22.850 33 \times 10^{-6})$
 Relative standard uncertainty: $u_{\text{PTB}} = 0.38 \times 10^{-9}$
 where u_{PTB} is calculated as the quadratic sum of $u_A = 0.31 \times 10^{-9}$ and, from Table 3, $u_B = 0.21 \times 10^{-9}$

6.2.b Possible influence of the cycle duration

In a similar investigation as the one described in Section 5.2.c, for the determination of $K1$ we did not find a significant dependence of ΔU on T_C , to a relative uncertainty of better than 1 part in 10^9 . The results of measurements with three different cycle durations are shown in Figure 4. Especially, there was no significant difference found between the ΔU results obtained for $T_C = 20$ s (standard case) or 80 s. We conclude that the effect of T_C is not significant within the uncertainty of the comparison.

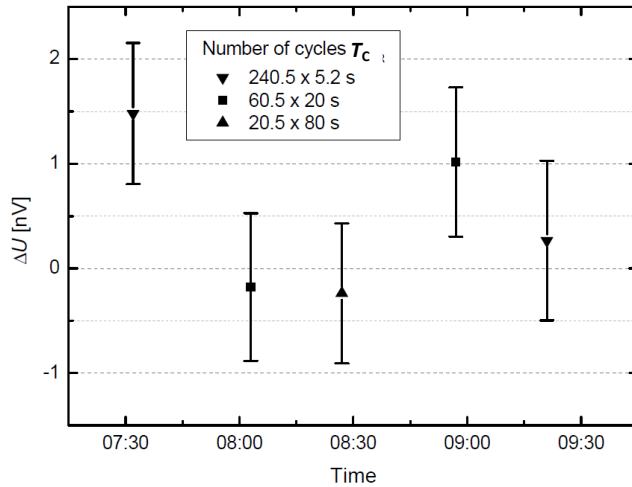


Figure 4: Average bridge voltage difference ΔU for a series of measurements with three different values for the cycle duration T_C . Again, an increase of ΔU by 1 nV corresponds to a decrease in the resistance ratio by 1 part in 10^9 . The type-A uncertainties are very close to those of the results presented in section 6.2.a.

6.3 Comparison of $K1$ measurements

No significant instabilities of the standards were detected and therefore no additional uncertainty component included in the final result.

From Table 6 and Table 7, the relative difference in the measurement $K1$ was found to be:

$$(K1_{PTB} - K1_{BIPM}) / K1_{BIPM} = + 0.7 \times 10^{-9}$$

Relative combined standard uncertainty: $u_{comp} = 1.9 \times 10^{-9}$

where u_{comp} is calculated as the quadratic sum of $u_{BIPM} = 1.9 \times 10^{-9}$ and $u_{PTB} = 0.38 \times 10^{-9}$

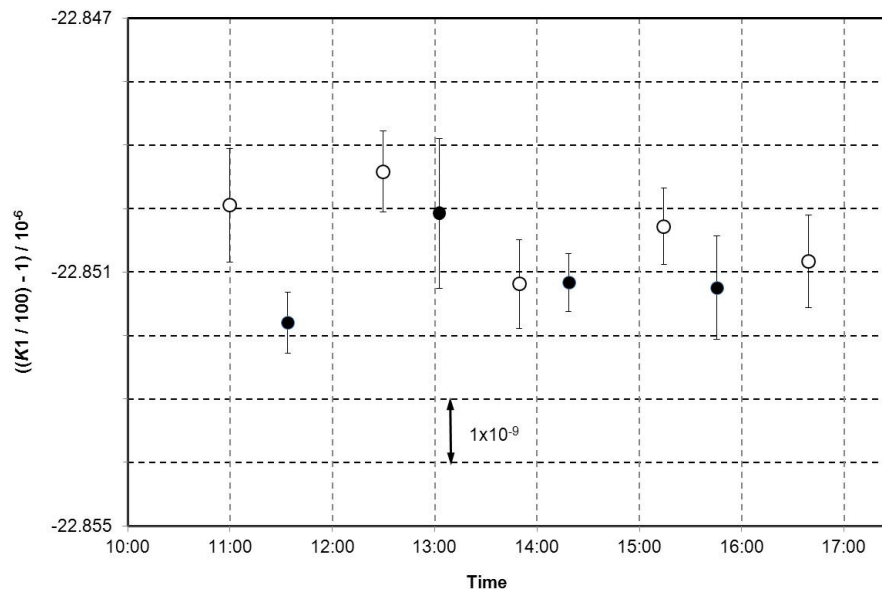


Figure 5: PTB (white circles) and BIPM (black dots) measurements of the ratio $K1$ ($10\,000\ \Omega/100\ \Omega$) on 18 November 2013. The uncertainty bars correspond to the dispersion observed during each measurement.

7 Measurements of the (100 Ω / 1 Ω) ratio K_2

7.1 Preliminary measurements

The measurements of the (100 Ω /1 Ω) ratio K_2 were carried out by both laboratories in a way similar to that used for the measurement of K_1 . The nominal current was 50 mA rms in 1 Ω .

The BIPM measurements at 1 Hz were corrected for a 1 Hz -‘dc’ difference of 17.6×10^{-9} , which is significantly larger than that corresponding to the K_1 ratio. These correction values are based on the comparison at the BIPM of the ratios measured alternately at 1 Hz, and at ‘dc’ (one full cycle takes about 340 s) using the BIPM CCC bridge.

The PTB used a cycle time $T_C = 20$ s with its CCC system.

A preliminary test was carried out on the 14 November, with four BIPM measurements interleaved with three PTB measurements. The relative difference was found to be:

$(K_{2PTB} - K_{2BIPM}) / K_{2BIPM} = +9.64 \times 10^{-9}$, with a combined standard uncertainty associated with the dispersion of the order of 1 part in 10^9 .

This large difference was not completely surprising: both laboratories were aware of the influence of the reversal time in the presence of a significant Peltier effect in low-value resistors.

This influence was already clearly identified during previous comparisons, in particular at NPL in 1997 [4], where one of the conclusions was: ‘*It was demonstrated that to limit the influence of the Peltier effect on the 100 Ω /1 Ω ratio measurement, it is essential that both laboratories use identical and sufficiently long delays after reversing the current in the dc measurements*’.

7.2 Investigations about cycle time

PTB carried out a first time-symmetric series of measurements with T_C varying from 5.2 s to 80 s and back. Results showed a reduction of the difference between the PTB results and the BIPM ‘dc’ corrected values when increasing T_C , but still no clear agreement.

The PTB decided therefore to carry out a systematic investigation covering a large range from 5.2 s to 320 s. For each cycle time T_C , the data acquisition started after a settling time equal to half of the plateau duration (i.e. $T_C/4$), with a sample interval of 20 ms.

The results are shown in Figure 6, together with the BIPM result at 1 Hz.

One additional PTB point is also included on the graph (white diamond) for $T_C = 80$ s with a 12 hour measurement time. It is worth to note that the low dispersion associated with $T_C = 320$ s was obtained from an overnight series lasting 14.5 hours.

It was expected that the influence of the Peltier effect would ‘saturate’ at both ends of the range. For cycle times much shorter than the time constant of the induced thermal emf, the Peltier effect is averaged to a value close to zero [6]. This is the interpretation of the ‘plateau’ seen for T_C smaller than 10 s. For T_C values much larger than the thermal time constant, the thermal effect should have enough time to reach a stable value corresponding to the maximum influence for a given experimental configuration. However, this second ‘plateau’ does not appear here, even for a T_C as large as 320 s.

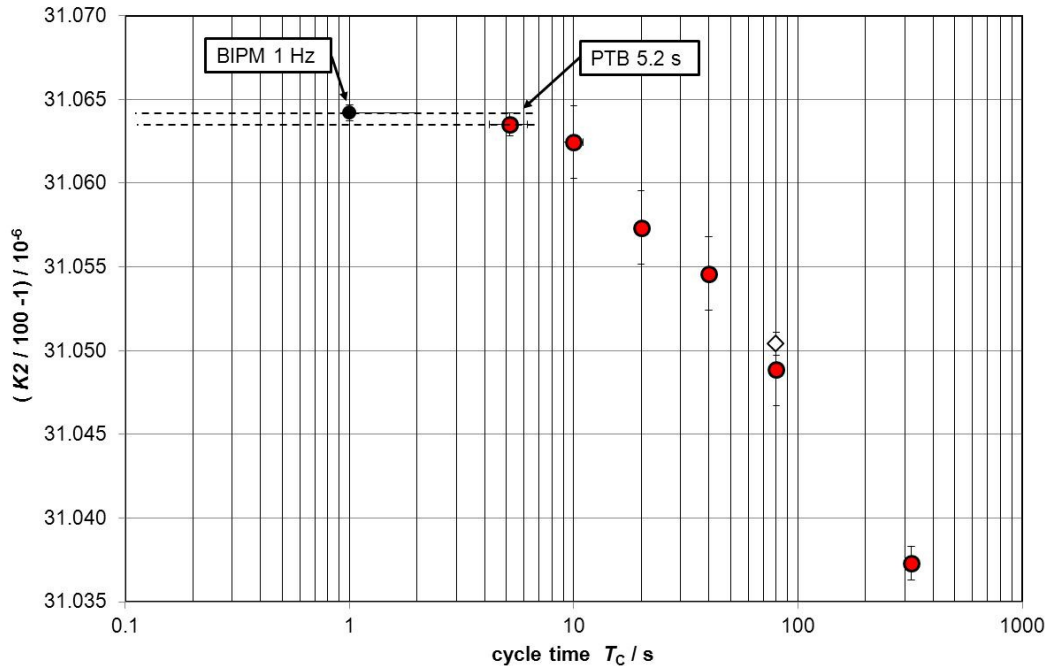


Figure 6: PTB (red circles) and BIPM (black dot) measurements of the $(100 \Omega/1 \Omega)$ ratio K_2 as a function of cycle duration.

The white diamond represents an additional measurement for $T_C = 80$ s with a 12 hour measurement time. The low dispersion associated with $T_C = 320$ s was obtained from an overnight series lasting 14.5 hours. The uncertainty bars correspond to dispersion only (type A).

7.3 Discussion

The absence of a saturation plateau for long cycle times may be the indication that the Peltier effect has not reached a ‘stable’ value even for a cycle time as long as 320 s, or that another unidentified effect of long time constant is present.

In any case, longer T_C values are still technically possible, but for the same type-A uncertainty the measurement time would have to be increased considerably to compensate for the rise of noise towards lower frequencies. Performing a series of interleaved measurements would finally become impractical, due to both the increased measurement time and the limited stability of the standards.

As a conclusion, the definition of ‘dc-resistance measurements’ as given in section 2 of this report cannot be fulfilled within the target uncertainties using this BIPM 1Ω standard, in the technical conditions of an on-site comparison.

7.4 Comparability of BIPM and PTB measurements of K_2

The aim of such on-site comparison is to demonstrate the equivalence of the results obtained by the two laboratories in the measurement of a same $(100 \Omega/1 \Omega)$ ratio of ‘dc resistance’.

In the present case, the conditions of ‘dc resistance’ are not sufficiently well-defined, given the resolution of the two measurement systems. But the equivalence of the measurement facilities can still be demonstrated for operating conditions being equivalent for both systems.

The choice of an equivalent long measurement cycle time seems difficult.

The shapes of the current signals are very different for each system. The BIPM CCC bridge includes zero-current steps before reversal, and the settling time of the current steps is of the order of 20 s. In

contrast, the PTB bridge produces short settling times (about 0.2 s), leading to an almost rectangular shape.

Consequently, it would be very difficult to determine which PTB reversal time would produce the same thermal behaviour in the 1 Ω standard as that produced by the BIPM CCC current.

The problem is less critical with the BIPM 1 Hz bridge: as seen on Figure 6 the 1 s period is close to the beginning of the ‘plateau’ starting at $T_C = 10$ s.

We suggest that the best equivalence of operating conditions was obtained when operating the BIPM bridge at 1 Hz without ‘dc’ correction, and the PTB bridge with $T_C = 5.2$ s.

This frequency range is high enough to average out the Peltier effect and still low enough to keep other ac effects to a negligible value.

It was therefore decided to carry out the comparison of (100 Ω/1 Ω) ratios under equivalent operating conditions, BIPM 1 Hz and PTB $T_C = 5.2$ s in the present case, and not as ratios of ‘dc-resistance’ values.

It was also concluded that more investigations should be carried out in the near future about the behaviour of 1 Ω resistance standards at operating frequencies close to ‘dc’. At the BIPM, reversal times of the order of 2 minutes were assumed to be close enough to ‘dc’ conditions. These results suggest that it is perhaps not the case.

Additional studies seem necessary to get a more accurate definition of the measurand for future comparisons of (100 Ω/1 Ω) ratios.

7.4 Influence on the uncertainty budget

When the 1 Hz bridge is no longer used as a transfer instrument referenced to the CCC, one has to take into account the uncertainty associated with the accuracy of its room-temperature current comparator and resistive divider [9]. See Table 8.

The assumption that the plateau corresponding to negligible residual Peltier effect is reached at $T_C = 5.2$ s is based on the shape of the curve on Figure 6, but more data would be useful in the region 1 s to 5s to get a better accuracy. A conservative relative standard uncertainty component to cover this assumption was estimated to be $u_{\text{Peltier}} = 3 \times 10^{-9}$.

Resistance ratio	100 Ω / 1 Ω
Relative standard uncertainties	/ 10 ⁻⁹
Room temperature current comp.	
Ratio error	1.0
Resistive divider calibration	0.5
Finite gain of servo	0.5
Combined $u_B =$	1.2

Table 8 : Uncertainty budget associated with the BIPM 1 Hz bridge for the measurement of (100 Ω/1 Ω) ratios.

7.5 BIPM and PTB measurements of K2

On the 21 November, four BIPM measurements of K2, interleaved with five PTB measurements, were performed using the operating conditions described in section 7.4.

Each BIPM result reported in Table 9 is the mean value of five individual measurements at 1 Hz, corresponding to a total integration time of about 26 minutes. The associated dispersion is estimated by the standard deviation of the mean of the five measurements.

Each PTB result reported in Table 10 is calculated from the data acquisition of 240 cycles (at $T_C = 5.2$ s), with the associated standard deviation of the mean.

Time	$(K2_{\text{BIPM}}/100) - 1$ / 10^{-6}	dispersion / 10^{-9}
8:33	31.0635	0.9
9:54	31.0642	0.3
11:16	31.0646	0.9
12:34	31.0647	1.0
mean value =	31.0642	
Std dev. of mean $u_A =$	0.3×10^{-9}	

Table 9: BIPM measurements at 1 Hz of the (100 Ω /1 Ω) ratio $K2$, on 21 November 2013.

No 'dc' correction applied. Results are expressed as the relative difference from the nominal value 100.

BIPM result: $K2_{\text{BIPM}} = 100 \times (1 + 31.0642 \times 10^{-6})$
 Relative standard uncertainty: $u_{\text{BIPM}} = 2.5 \times 10^{-9}$
 where u_{BIPM} is calculated as the quadratic sum of
 $u_A = 0.3 \times 10^{-9}$ and, from Table 8 $u_B = 1.2 \times 10^{-9}$

Time	$(K2_{\text{PTB}}/100) - 1$ / 10^{-6}	dispersion / 10^{-9}
7:31	31.0654	1.7
9:13	31.0626	1.4
10:34	31.0631	1.7
11:52	31.0634	1.7
13:09	31.0627	0.9
mean value =	31.0635	
Std dev. of the mean =	0.7×10^{-9}	

Table 10 : PTB measurements of the (100 Ω /1 Ω) ratio $K2$, on 21 November 2013. Cycle time: 5.2 s. Results are expressed as the relative difference from the nominal value 100.

PTB result: $K2_{\text{PTB}} = 100 \times (1 + 31.0635 \times 10^{-6})$
 Relative standard uncertainty: $u_{\text{PTB}} = 0.95 \times 10^{-9}$
 where u_{PTB} is calculated as the quadratic sum of
 $u_A = 0.7 \times 10^{-9}$ and, from Table 3, $u_B = 0.65 \times 10^{-9}$

7.6 Comparison of $K2$ measurements

No significant instabilities of the standards were detected and therefore no additional uncertainty component included in the final result.

The relative difference PTB – BIPM in the measurement $K2$ was found to be:

$$(K2_{\text{PTB}} - K2_{\text{BIPM}}) / K2_{\text{BIPM}} = -0.8 \times 10^{-9}$$

Relative combined standard uncertainty: $u_{\text{comp}} = 4.0 \times 10^{-9}$

where u_{comp} is calculated as the quadratic sum of
 $u_{\text{BIPM}} = 2.5 \times 10^{-9}$, $u_{\text{PTB}} = 0.95 \times 10^{-9}$, and $u_{\text{Peltier}} = 3 \times 10^{-9}$

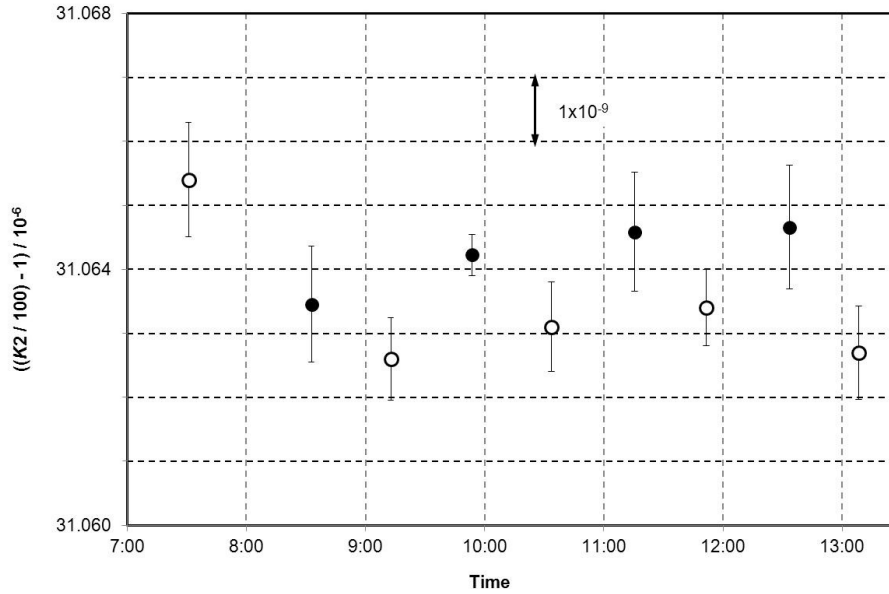


Figure 7: BIPM measurements at 1 Hz (black dots) and PTB measurements (white circles, cycle time: 5.2 s) of the (100 Ω/1 Ω) ratio $K2$, on 21 November 2013.

8 Conclusion

The bilateral on-site comparison BIPM-PTB carried out in November 2013 showed an excellent agreement in the measurement of a conventional 100 Ω standard resistor in terms of the quantized Hall resistance, and in the determination of the resistance ratios of nominal values $K1 = (10\,000\ \Omega/100\ \Omega)$ and $K2 = (100\ \Omega/1\ \Omega)$. These results are summarized in Table 11.

Each time, the relative difference was found to be smaller than 1 part in 10^9 .

For the measurement of the 100 Ω resistor and the ratio $K1$, the standard uncertainty of the comparison is of the order of 2 parts in 10^9 .

For the ratio $K2$, careful experimental tests showed that the conditions of ‘dc resistance’ measurements were not sufficiently well-defined with the 1 Ω standard used, most likely due to a Peltier effect. The experimental conditions had therefore to be slightly modified, and an uncertainty component associated with the Peltier effect was added. Under these experimental conditions, the standard uncertainty of the comparison of $K2$ is 4 parts in 10^9 .

These results also show that more investigations should be carried out on the behaviour of low-value resistors in the frequency regime below 1 Hz. More generally, discussions should take place within the metrology community about the notion of ‘dc resistance’, both for general work in metrology and for clearly defined measurands in future on-site comparisons.

$R_{100\Omega}$ in terms of $R_H(2)$	$(R_{PTB} - R_{BIPM}) / R_{BIPM} = -0.5 \times 10^{-9}$	$u_{comp} = 2.2 \times 10^{-9}$
$K1 = R_{10k\Omega} / R_{100\Omega}$	$(K1_{PTB} - K1_{BIPM}) / K1_{BIPM} = +0.7 \times 10^{-9}$	$u_{comp} = 1.9 \times 10^{-9}$
$K2 = R_{100\Omega} / R_{1\Omega}$	$(K2_{PTB} - K2_{BIPM}) / K2_{BIPM} = -0.8 \times 10^{-9}$	$u_{comp} = 4.0 \times 10^{-9}$

Table 11 : Results of the BIPM-PTB comparison, and their associated relative standard uncertainties. The measurements of $K2$ were carried out at 1 Hz without ‘dc’ correction by the BIPM and with a cycle time of 5.2 s by the PTB.

The results will also appear as Degrees of Equivalence (DoE) in the BIPM Key Comparison Database (KCDB).

The DoE of a laboratory with respect to the reference value is given by a pair of terms: the difference D from the reference value and its expanded uncertainty ($k = 2$), $U = 2 u$.

The reference value of the on-going comparison BIPM.EM-K12 was chosen to be the BIPM value.

The comparison results expressed as DoEs are summarized in Table 12.

	Degree of equivalence $D / 10^{-9}$	Expanded uncertainty $U / 10^{-9}$
$R_{100\Omega}$ in terms of $R_H(2)$	- 0.5	4.4
$K1 = R_{10k\Omega} / R_{100\Omega}$	+ 0.7	3.8
$K2 = R_{100\Omega} / R_{1\Omega}$	- 0.8	8.0

Table 12 : Comparison results expressed as degrees of equivalence: difference from the BIPM reference value and expanded uncertainty ($k = 2$).

-
- 1 Delahaye F., Witt T. J., Piquemal F., Genevès G., *IEEE Trans. Instrum. Meas.*, 1995, **44**, 258-261.
 - 2 Delahaye F., Witt T. J., Jeckelmann B., Jeanneret B., *Metrologia*, 1995/96, **32**, 385-388.
 - 3 Delahaye F., Witt T. J., Pesel E., Schumacher B., Warnecke P., *Metrologia*, 1997, **34**, 211-214.
 - 4 Delahaye F., Witt T.J, Hartland A., Williams J.M., Rapport BIPM-99/18
 - 5 Delahaye F., Witt T.J, Elmquist R.E., Dziuba R.F., *Metrologia*, 2000, **37**, 173-176
 - 6 Delahaye F., *Metrologia*, 1992, **29**, 81
 - 7 Delahaye F., *IEEE Trans. Instrum. Meas.*, 1991, **40**, 6, 883-888.
 - 8 T J B M Janssen, J M Williams, N E Fletcher, R Goebel, A Tzalenchuk, R Yakimova, S Lara-Avila, S Kubatkin and V I Fal'ko, *Metrologia*, 2012 , **49**, 294
 - 9 Delahaye F., Bournaud D., *IEEE Trans. Instrum. Meas.*, 1993, **42**, 287-291.
 - 10 Delahaye F., Bournaud D., *IEEE Trans. Instrum. Meas.*, 1991, **40**, 237-240.
 - 11 M. Götz, D. Drung, E. Pesel, H.-J. Barthelmess, C. Hinnrichs, C. Aßmann, M. Peters, H. Scherer, B. Schumacher, and T. Schurig, *IEEE Trans. Instrum. Meas.*, 2009, **58**, 1176-1182.
 - 12 D. Drung and J.-H. Storm, *IEEE Trans. Instrum. Meas.*, 2011, **60**, 2347-2352.
 - 13 D. Drung, M. Götz, E. Pesel, H.-J. Barthelmess, and C. Hinnrichs, *IEEE Trans. Instrum. Meas.*, 2013, **62**, 2820-2827.
 - 14 M. Götz, D. Drung, E. Pesel, and F.-J. Ahlers, *IEEE Trans. Instrum. Meas.*, 2011, **60**, 2660-2666.
 - 15 Delahaye F. and Jeckelmann B., *Metrologia*, 2003, **40**, 217-223.
 - 16 K. Pierz and B. Schumacher, *IEEE Trans. Instrum. Meas.*, 1999, **48**, 293-295.
 - 17 K. Pierz, M. Götz, E. Pesel, F.-J. Ahlers, and H.W. Schumacher, *IEEE Trans. Instrum. Meas.*, 2011, **60**, 2455-2461.
 - 18 F. Delahaye, *Metrologia*, 1989, **26**, 63-68.